Title
Effect of vocal fold stiffness on voice production in a three-dimensional body-cover phonation model

Journal
The Journal of the Acoustical Society of America, 142(4)

ISSN
0001-4966

Author
Zhang, Zhaoyan

Publication Date
2017-10-01

DOI
10.1121/1.5008497

Peer reviewed

Effect of vocal fold stiffness on voice production in a three-dimensional body-cover phonation model

Zhaoyan Zhang[a)]
Department of Head and Neck Surgery, University of California, Los Angeles, 31-24 Rehabilitation Center, 1000 Veteran Avenue, Los Angeles, California 90095-1794, USA

(Received 22 February 2017; revised 26 September 2017; accepted 5 October 2017; published online 24 October 2017)

Although stiffness conditions in the multi-layered vocal folds are generally considered to have a large impact on voice production, their specific role in controlling vocal fold vibration and voice acoustics is unclear. Using a three-dimensional body-cover continuum model of phonation, this study shows that changes in vocal fold stiffness have a large effect on F0 and the means and amplitudes of the glottal area and flow rate. However, varying vocal fold stiffness, particularly along the anterior–posterior direction, has a much smaller effect on the closed quotient, vertical phase difference, and the spectral shape of the output acoustics, which are more effectively controlled by changes in the vertical thickness of the medial surface. These results suggest that although changes in vocal fold stiffness are often correlated with production of different voice types, there is no direct cause–effect relation between vocal fold stiffness and voice types, and the correlation may simply result from the fact that both vocal fold stiffness and geometry are regulated by the same set of laryngeal muscles. These results also suggest the possibility of developing reduced-order models of phonation in which the vocal fold is simplified to a one-layer structure.
 https://doi.org/10.1121/1.5008497

[LK] Pages: 2311–2321

I. INTRODUCTION

Vocal folds are layered structures, consisting of an inner muscular layer, a soft tissue layer of the lamina propria, and an outmost epithelium layer. The lamina propria is often divided into a superficial, an intermediate, and a deep layer based on the distribution of collagen and elastin fibers (Hirano, 1974; Gray, 2000). This histological difference leads to different mechanical properties across these layers. While the mechanical properties of the vocal fold have an obvious role in regulating phonation frequency (F0), the difference in mechanical properties across layers has been hypothesized to also play an important role in determining vocal fold vibration and the resulting voice quality. In the body-cover theory of phonation (Hirano, 1974; Hirano and Kakita, 1985), in which the body layer includes the muscular layer and the deep layer of the lamina propria and the cover layer includes all the other outer layers, Hirano argued that four typical voice types can be produced by laryngeal adjustments involving primarily the cricothyroid (CT) and thyroarytenoid (TA) muscles, which lead to differential stiffness conditions in the body and cover layers, particularly along the anterior–posterior (AP) direction. These four voice types differ in the vibration amplitudes of the body and cover layers, the appearance of a wave-like motion on the vocal fold surface or a vertical phase difference in vocal fold motion along the medial surface, pitch and loudness ranges, and voice quality registration (e.g., modal vs falsetto).

Although the body-cover theory of phonation is widely adopted in the voice literature, the cause–effect relation between the body-cover stiffness conditions and the corresponding voice types produced has not been directly validated, probably due to difficulties in *in vivo* measurement of the mechanical properties of each layer. On the other hand, because contraction of laryngeal muscles that are responsible for the control of vocal fold stiffness also leads to significant changes in vocal fold geometry, it still remains unclear whether the differences between the four voice types discussed in Hirano (1974) are mainly due to changes in vocal fold stiffness or geometry or a combination of both. In particular, the two laryngeal muscles that regulate vocal fold stiffness, the CT and TA muscles, also have a large influence on the vertical thickness of the vocal folds, which has been hypothesized to have a large impact on the glottal closure pattern and voice quality (van den Berg and Tan, 1959; van den Berg, 1968). This important role of the vertical thickness of the vocal folds was confirmed in a recent computational study (Zhang, 2016), which showed that the vertical thickness had a dominant effect on the glottal closure pattern and the spectral shape of the output acoustics. In contrast, Zhang (2016) also showed that, other than regulating phonation frequency, vocal fold stiffness had a minimal effect on the glottal closure and the spectral shape of the output acoustics, except for extreme conditions of very low vocal fold stiffness and very low subglottal pressures.

One important limitation of the Zhang (2016) study is that a one-layer vocal fold model was used and only changes in vocal fold stiffness along the AP direction were considered. One may wonder if vocal fold stiffness may play a more important role in a multi-layered setting, as hypothesized in the body-cover theory of phonation. The goal of this study is to clarify the possible roles of vocal fold stiffness in

[a)]Electronic mail: zyzhang@ucla.edu

regulating voice production, specifically its roles in regulating the glottal closure pattern and the spectral shape of the output acoustics, in a two-layer vocal fold model.

A better understanding of the roles of vocal fold stiffness in the control of the output voice spectra has both theoretical and practical importance. Vocal folds are known to exhibit nonlinear, anisotropic material properties, which are difficult to quantify experimentally. A better understanding of the effect of vocal fold stiffness on phonation would identify the aspects of material properties that are of importance to voice production and thus need to be better quantified experimentally. It would also facilitate the development of reduced-order models of phonation in which these important aspects are better represented and other less important aspects are simplified or neglected completely. Clinically, such understanding would allow clinicians to focus on mechanical properties that are of perceptual importance and should be targeted for restoration in the management of voice disorders.

This study uses the same computational model as used in Zhang (2016), but extends it to a body-cover two-layer model. The AP stiffness in both the body and cover layers and the transverse stiffness (stiffness within the coronal plane) are varied and their effects on vocal fold vibration and voice acoustics are investigated. In the following, the model and data analysis methods are first described in Sec. II. The effect of the transverse and AP stiffnesses on voice production is presented in Sec. III. The implications of the results are discussed in Sec. IV.

II. METHOD

A. Numerical model and simulation conditions

Figure 1 shows the three-dimensional vocal fold model used in this study. Although two folds are shown in the figure, left-right symmetry in vocal fold properties (geometry, material properties, and position) and vibration about the glottal midline is imposed so that only one vocal fold is modeled in this study. The vocal fold is 17 mm long along the anterior–posterior direction. The posterior cross-sectional geometry of the vocal fold model is defined similarly to that in Zhang (2009, Fig. 2) and a sketch is also shown in Fig. 1. The depths (dimension along the medial−-lateral direction) of the body and cover layers are 6 and 1.5 mm, respectively, with a total depth of 7.5 mm. The cover layer depth is similar to that used in Titze and Talkin (1979), but is slightly larger than that reported in our recent measurement (about 1 mm; Wu and Zhang, 2016). The vertical thickness of the medial surface T in the inferior−superior direction is variable, as listed in Table I. The cover layer thickness at the lateral boundary is set to 1.5 mm, except for conditions with $T = 1$ and 2 mm, in which case the lateral thickness of the cover layer is reduced to 0.5 and 1.0 mm, respectively, in order to maintain the desired body layer depth of 6 mm. Note that once the vertical thickness T, the body and cover depths, and the cover layer lateral thickness are specified, the vertical thickness of the body layer medial surface and the inferior angles (α_{2b}, α_{2c}) are fully determined. The vocal fold cross-section tapers quadratically toward the anterior direction, with the total depth reduced to 6.56 mm in the middle coronal plane and 3.75 mm at the anterior surface of the vocal folds. This tapering leads to a continuously reduced body-layer depth along the AP direction while the cover layer depth remains constant at 1.5 mm (Fig. 1). Specifically, the three-dimensional vocal fold geometry is obtained by first extruding the posterior surface along the AP direction for 17 mm and then sectioning off the lateral portion of the resulting object by a vertical quadratically curved surface whose shape is determined by the total depths of the posterior surface, middle coronal surface, and the anterior surface. The medial surfaces of the two vocal folds form an angle α, changes in which control the resting glottal opening or degree of vocal fold approximation. The vocal fold model is fixed at the lateral surface and the two side surfaces at the anterior and posterior ends. No sub- or supra-glottal tracts are included in this study in order to avoid possible source−tract interaction.

The glottal fluid−structure interaction is modeled similarly to that in Zhang (2015, 2016). The reader is referred to these two papers for details of the model. Briefly, each vocal fold layer is modeled as a transversely isotropic, nearly incompressible, linear material with a plane of isotropy perpendicular to the AP direction (Itskov and Aksel, 2002). The material control parameters for each vocal fold layer include the transverse Young's modulus E_t, the AP Young's modulus E_{ap}, the AP shear modulus G_{ap}, and density. The density of the vocal fold is assumed to be 1030 kg/m^3. The AP Poisson's ratio is assumed to be 0.495. To reduce the number of conditions to be investigated, $E_{ap} = 4\,G_{ap}$ is also assumed, as in Zhang (2016), and the transverse Young's moduli of

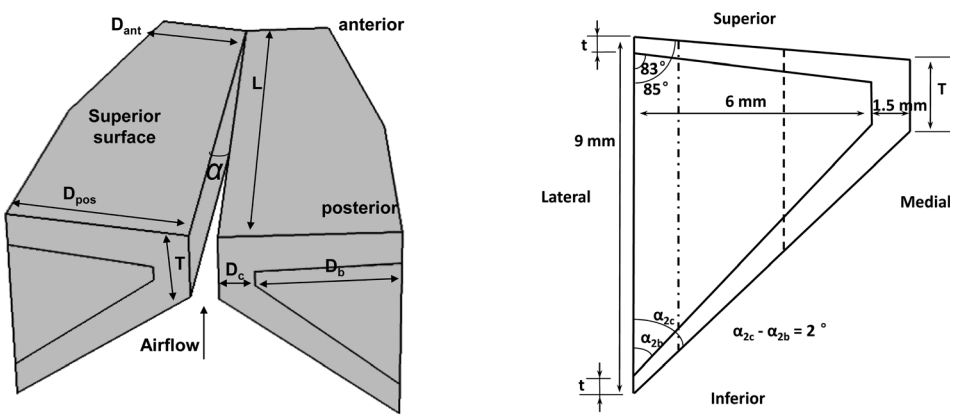

FIG. 1. The three-dimensional vocal fold model (left) and the geometry of the posterior surface (right). The body-layer depth reduces quadratically toward the anterior surface. The dash-dotted and dashed lines in the right panel indicate the lateral boundary of the vocal fold in the middle coronal plane and the anterior surface, respectively.

TABLE I. Ranges of simulation parameters. For all conditions, the vocal fold density is 1030 kg/m^3, the AP Poisson's ratio is 0.495, and $E_{ap} = 4\ G_{ap}$ is assumed.

Transverse stiffness	$E_t = [1, 2, 4]$ kPa
AP stiffness	See Table II
Vertical thickness	T = [1, 2, 3, 4.5] mm
Initial glottal angle	$\alpha = [0°, 1.6°, 4°]$
Subglottal pressure	$P_s = 50-2400$ Pa (18 conditions)

the two layers are assumed to be identical in the present study. The simplification of identical body-cover transverse stiffness is based on the numerical finding in Yin and Zhang (2013) which showed that the transverse stiffnesses in the body and cover layers were generally of the same order of magnitude across a large range of CT/TA activation conditions. Thus, the mechanical properties of the two-layer vocal fold are determined by three remaining moduli: the transverse Young's modulus $E_{t,}$ the cover-layer AP shear modulus $G_{apc,}$ and the body-layer AP shear modulus G_{apb}. For both layers, a constant loss factor of 0.4 is used, similar to Zhang (2015, 2016). The glottal flow is modeled as a one-dimensional quasi-steady glottal flow model. While it was neglected in Zhang (2015, 2016), the viscous loss in the glottal flow is included in this study by adding an extra pressure loss term in the one-dimensional flow equation, similar to Pelorson *et al.* (1994) but assuming an elliptical cross-section of the glottis (White, 1991),

$$\Delta P_{\text{viscous}} = Q\mu \int_z \left(\frac{4}{{L_g}^2 A_g} + \frac{\pi^2 {L_g}^2}{{A_g}^3} \right) dz, \tag{1}$$

where μ is the dynamic viscosity of air, Q is the instantaneous glottal flow rate, A_g is the instantaneous glottal area, and L_g is the glottal length. The integration in Eq. (1) is along the glottal channel from glottal inlet to the point of flow separation from the vocal fold surface.

While these simplifications are necessary for a large-scale parametric investigation as in this study, our previous studies using similar computational models have been able to reproduce experimental observations regarding sound production by confined pulsating jet flows (Zhang *et al.*, 2002), dependence of phonation threshold pressure on vocal fold properties (Farahani and Zhang, 2016), and vocal fold vibration patterns in different vibratory regimes and transitions between regimes (Zhang and Luu, 2012).

In this study, simulations are performed with parametric variations in the medial surface thickness, resting glottal angle, subglottal pressure, and the three material moduli (E_t, $G_{apb,}$ G_{apc}). Four values of medial surface thickness (1, 2, 3, and 4.5 mm) are considered, as in Zhang (2016). Because the effect of the resting glottal angle has been extensively investigated in Zhang (2016), only three values of the resting glottal angle (0°, 1.6°, and 4°) are considered in this study. The subglottal pressure is varied from 0.05 to 2.4 kPa, in 18 steps, as in Zhang (2016). The range of vocal fold stiffness is selected to encompass ranges used in previous numerical studies (e.g., Alipour *et al.*, 2000; Berry *et al.*, 1994). Three values of the transverse Young's modulus E_t are considered: 1, 2, and 4 kPa. For the AP shear modulus, five values are considered for each layer: 1, 10, 20, 30, and 40 kPa, which produces 25 combinations of AP stiffness conditions. For convenience, these 25 conditions are referred to by a G_{ap} index, with the correspondence between the index and the specific ($G_{apb,}$ G_{apc}) values given in Table II. In total 16 200 conditions are investigated. For each condition, the simulation was run for 0.5 s at a sampling rate of 44 100 Hz, with the subglottal pressure linearly increased from zero to a target value in 30 time steps and then kept constant.

B. Output measures

Data analysis as described in Zhang (2016) is performed using the last 0.25 s of each simulation by which time vocal fold vibration has reached steady-state or nearly steady-state. The output measures of vocal fold vibration include the mean glottal area $Ag_{0,}$ mean glottal flow rate Q_{mean}, glottal area amplitude Ag_{amp} (half of the difference between maximum and minimum glottal areas), glottal flow amplitude Q_{amp} (half of the difference between maximum and minimum glottal flow rates), closed quotient (CQ) (the duration of glottal closure as a fraction of the vibration period), and the vertical phase difference (VPD) (the phase difference in the medial−lateral motion between the upper and lower margins of the medial surface in the coronal plane). The output acoustic measures include the phonation frequency F0, A-weighted sound pressure level (SPL), and several spectral shape measures including H1−H2 (the amplitude difference between the first harmonic and the second harmonic), H1−H4 (the amplitude difference between the first harmonic and the fourth harmonic), H1−H2k (the amplitude difference between the first harmonic and the harmonic nearest 2 kHz), H1−H5k (the amplitude difference between the first harmonic and the harmonic nearest 5 kHz). These acoustic measures have been shown to be of perceptual importance (e.g., Klatt and Klatt, 1990). The reader is referred to Zhang (2016) for details of the extraction of these output measures.

C. Probabilistic-based global cause−effect analysis

Considering the potentially strong interactions between physiologic control parameters and the large amount of data available, it is of interest to identify significant effects of a specific control parameter that are consistent in a large range of vocal fold conditions. In this study, the global importance of specific control parameters to voice production will be evaluated in a probabilistic-based framework. Specifically,

TABLE II. The AP stiffnesses in the body and cover layers in the 25 AP stiffness conditions investigated.

G_{ap} Index	G_{apc} (kPa)	G_{apb} (kPa)
1−5	1	1, 10, 20, 30, 40
6−10	10	1, 10, 20, 30, 40
11−15	20	1, 10, 20, 30, 40
16−20	30	1, 10, 20, 30, 40
21−25	40	1, 10, 20, 30, 40

for each physiologic control parameter and each output measure, the probability of a certain amount of change in the specific acoustic measure due to changes in the physiologic control parameter of interest will be calculated. For example, consider the cause–effect relationship between the transverse stiffness E_t and the acoustic measure H1−H2. For each of the three values of the *Et,* parametric variation of other parameters (three resting glottal gaps, four vertical thicknesses, 18 subglottal pressures, and 25 shear modulus conditions) will lead to 5400 conditions. For each of the 5400 conditions, the change in H1−H2 as the transverse Young's modulus *Et* increases from the lowest (1 kPa) to the highest value (4 kPa) will be calculated. This will generate a set of 5400 changes in H1−H2, from which a histogram X will be generated as the distribution of the change in H1−H2 due to an *Et* increase across the 5400 conditions. Following the same procedure, a histogram will be generated for changes in each output measure due to increases in each of the physiologic control parameters.

For each histogram distribution X, a mean value M and a skewness factor S are calculated as below,

$$M = \sum_{1}^{N} X/N \ ,$$
$$S_1 = -\sum X^+ \Big/ \sum X^-,$$
$$S = \begin{cases} S_1, & S_1 >= 1 \\ -1/S_1, & S_1 < 1, \end{cases} \tag{2}$$

where N is the number of samples in the distribution X, and X^+ and X^- are subsets of X consisting of samples of positive and negative values, respectively. The mean value M quantifies the average expected change in the output measure due to increases in a specific control parameters. The absolute value of the skewness factor S, the ratio between the sums of samples in X^+ and X^-, quantifies the likelihood that an increase in a control parameter produce a consistently positive or consistently negative change in an output measure, whereas the sign of S indicates the direction of change in the output measure (i.e., an increase or decrease in the output measure). An absolute value of S much larger than 1 indicates that an increase in the corresponding control parameter is very likely to cause the output measure to change toward one consistent direction (either increase or decrease), independent of values of other control parameters. For example, a histogram with $S = -10$ indicates that an increase in the corresponding control parameter has about 90% probability to reduce the corresponding output measure. In contrast, a small absolute value of S indicates that the effect of the control parameter on the output measure is highly dependent on other control parameters, and can be either positive or negative.

For each output measure, the M and S values of the histograms relating physiologic control parameters to this specific output measure will be compared across each other. This will identify the physiologic control parameters that have a significant effect on the output measure of interest. On the other hand, comparison of histograms relating the same physiologic control parameter to various output measures will identify its most significant effect on voice production. In this study, a control parameter is considered to have a significant effect on an output measure if the absolute value of S is larger than 5 and the M value is dominant when compared to those of other control parameters.

III. RESULTS

In general, the effects of the vertical thickness of the medial surface, resting glottal angle, and subglottal pressure are similar to those observed in Zhang (2016), and are thus only described briefly in this study. The following focuses mainly on the effects of vocal fold stiffness.

A. Phonation at isotropic or near-isotropic conditions

For conditions with G_{ap} index 1–5, in which the G_{apc} is very small at 1 kPa, the vocal fold cover layer is under either isotropic or near-isotropic stiffness conditions (i.e., AP stiffness is comparable to the transverse stiffness), particularly for conditions with $E_t = 4$ kPa. Vocal folds under such conditions exhibit qualitatively different vocal fold vibration patterns from anisotropic vocal folds (G_{ap} index 6−25), similar to experimental observations in self-oscillating physical vocal fold models (Thomson *et al.,* 2005; Zhang *et al.,* 2006; Murray and Thomson, 2012; Xuan and Zhang, 2014). Specifically, the vocal folds exhibit large vertical motion and the medial surface often takes on a divergent profile during almost the entire vibration cycle, rather than an alternatingly convergent–divergent shape as often observed in human phonation. Phonation under such isotropic or near-isotropic conditions often requires a very high threshold subglottal pressure, as shown in Fig. 2. In fact, in most of such isotropic or near-isotropic conditions phonation is not observed during the subglottal pressure range investigated, particularly for conditions with $E_t = 4$ kPa.

Note that vocal folds under these isotropic or near-isotropic conditions generally exhibit large vocal fold deformation, which may have violated the linear elasticity assumption made in our computational model. In addition, these conditions generally do not occur in human phonation. Thus, in the following, data obtained under these conditions are included only for completeness but are not discussed in detail.

B. Phonation threshold pressure

Figure 2 shows the phonation threshold pressure as a function of G_{ap} Index, for conditions of different transverse stiffnesses, vertical thicknesses and resting glottal angles. Note that the G_{ap} index is scaled in such a way so that the AP stiffnesses vary with increasing G_{ap} index in groups of five (Table II), with each group consisting of conditions with identical values of the cover-layer AP stiffness but increasing body-layer AP stiffness. As a result, the phonation threshold pressure shows a variation pattern with increasing G_{ap} index in groups of five along the G_{ap} index axis in Fig. 2 (e.g., in the rightmost panels of the top and bottom rows).

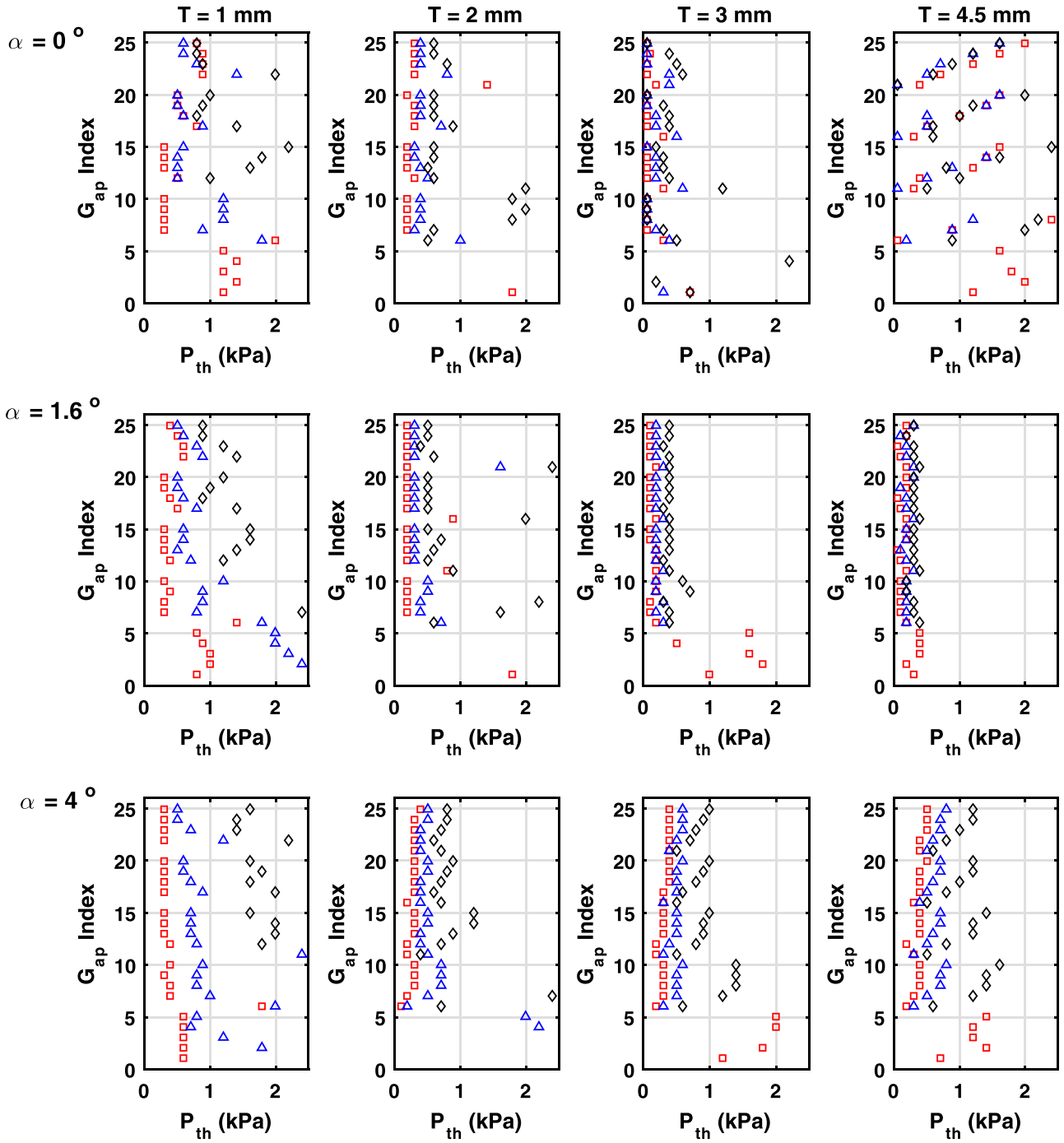

FIG. 2. (Color online) Phonation threshold pressure as a function of the AP stiffness (as indicated by the G_{ap} Index) for different conditions of the transverse stiffness E_t, vertical thickness of the medial surface T, and resting glottal angle α. □, $E_t = 1$ kPa; △, $E_t = 2$ kPa; ◇, $E_t = 4$ kPa. Note that the G_{ap} index is scaled in such a way so that the AP stiffnesses vary with increasing G_{ap} index in groups of five (Table II), and the effects of increasing body-layer AP stiffness are demonstrated by the within-group variations, whereas the effects of increasing cover-layer AP stiffness are demonstrated by cross-group variations.

Thus, the effects of increasing body-layer AP stiffness are demonstrated by the within-group variations, whereas the effects of increasing cover-layer AP stiffness are demonstrated by cross-group variations.

For anisotropic stiffness conditions (i.e., G_{ap} Index 6–25, for which AP stiffness is larger than the transverse stiffness), the phonation threshold pressure is generally lowest at an intermediate resting glottal angle ($\alpha = 1.6°$). A larger resting glottal angle of 4° reduces the glottal fluid-structural coupling strength (Zhang, 2010), which leads to increased phonation threshold pressure when compared to conditions with $\alpha = 1.6°$. A smaller resting glottal angle of 0° increases the viscous dissipation in the airflow, thus also increasing phonation threshold pressure (particularly for T = 4.5 mm). Similarly, vocal folds with a vertical thickness T = 1 mm generally have a glottal area that is much larger than the resting glottal area and thus a high phonation threshold pressure. Similar to Zhang (2016), increasing vertical thickness T has a non-monotonic effect on the phonation threshold pressure, with the lowest threshold pressure reached generally at an intermediate value (T = 3 mm).

In general, increasing the transverse stiffness E_t consistently increases the phonation threshold pressure, particularly for conditions with a large resting glottal gap. Increasing the AP stiffness in the cover layer generally has a much smaller effect, when conditions of $G_{apc} = 1$ kPa are excluded from consideration. In contrast, the effect of increasing AP stiffness in the body layer (G_{apb}) on phonation threshold pressure is more complex. For conditions with large resting glottal angles ($\alpha = 4°$) and large vertical thicknesses ($T > 1$ mm), increasing body-layer AP stiffness generally increases the phonation threshold pressure. For conditions with a small vertical thickness (e.g., $T < 4.5$ mm) and a resting glottal angle $\alpha = 0°$, increasing body-layer AP stiffness decreases the phonation threshold pressure. For intermediate conditions (e.g., $\alpha = 1.6°$ and $T > 1$ mm), the effect of varying body-layer AP stiffness is generally small. A strong interaction between the body-layer AP stiffness and the transverse stiffness is also observed, with the effect of the body-layer AP stiffness significantly larger at conditions with a high transverse stiffness (e.g., $E_t = 4$ kPa, bottom row of Fig. 2).

The complex pattern of the dependence of the phonation threshold pressure on vocal fold stiffness is probably due to the effect of the transverse and AP stiffnesses on the frequency spacing between vocal fold eigenmodes (Berry, 2001), which is an important factor affecting the phonation threshold pressure (Zhang, 2010). On the other hand, increasing stiffness also reduces the mean glottal area significantly at some conditions (see below), which enhances vocal fold-airflow coupling and lowers the phonation threshold pressure. Viscous flow dissipation may also play an important role in conditions with a very small glottal area (e.g., large thicknesses and small resting glottal angles). The overall effect of stiffness on the phonation threshold pressure thus depends on the relative strength of these different mechanisms.

C. Vocal fold vibration, glottal flow, and output acoustics

Figure 3 shows different output measures of vocal fold vibration, glottal flow, and acoustics as a function of the G_{ap} index, subglottal pressure, and vertical thickness, for conditions of $E_t = 1$ kPa and $\alpha = 0°$. The effects of the vertical thickness and the subglottal pressure are similar to those observed in Zhang (2016). The following thus focuses on the effects of vocal fold stiffness. Note again that because of the way the G_{ap} index is scaled with the AP stiffnesses, most of the output measures show a variation pattern with increasing G_{ap} index in groups of five along the G_{ap} index axis in Fig. 3,

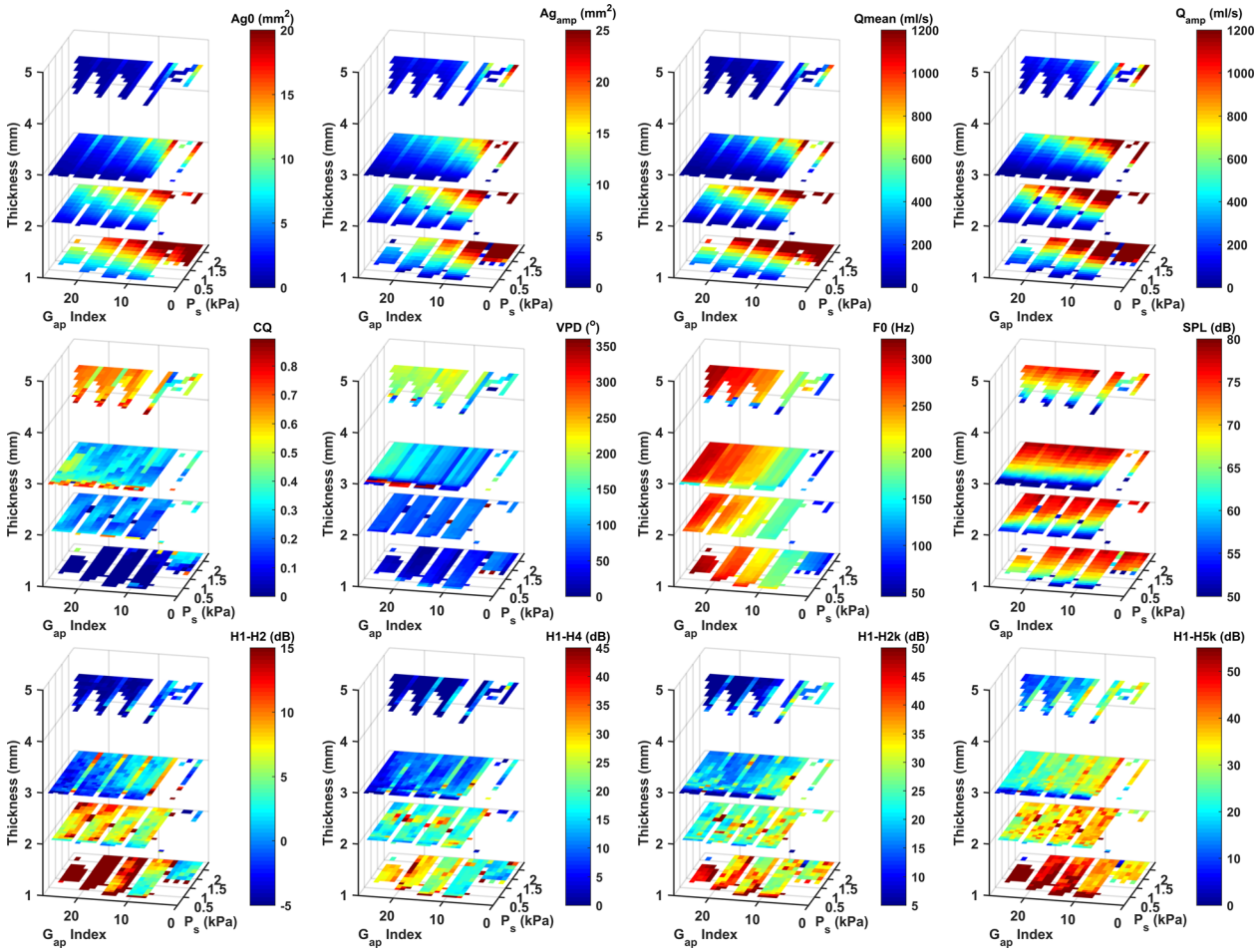

FIG. 3. (Color online) Effects of the AP stiffness (as indicated by the G_{ap} Index) on selected output measures. $E_t = 1$ kPa, $\alpha = 0°$. See Sec. II for definitions of different output measures. The region without data indicates conditions at which no phonation was observed. Note that the G_{ap} index is scaled in such a way so that the AP stiffnesses vary with increasing G_{ap} index in groups of five (Table II), and the effects of increasing body-layer AP stiffness are demonstrated by the within-group variations, whereas the effects of increasing cover-layer AP stiffness are demonstrated by cross-group variations.

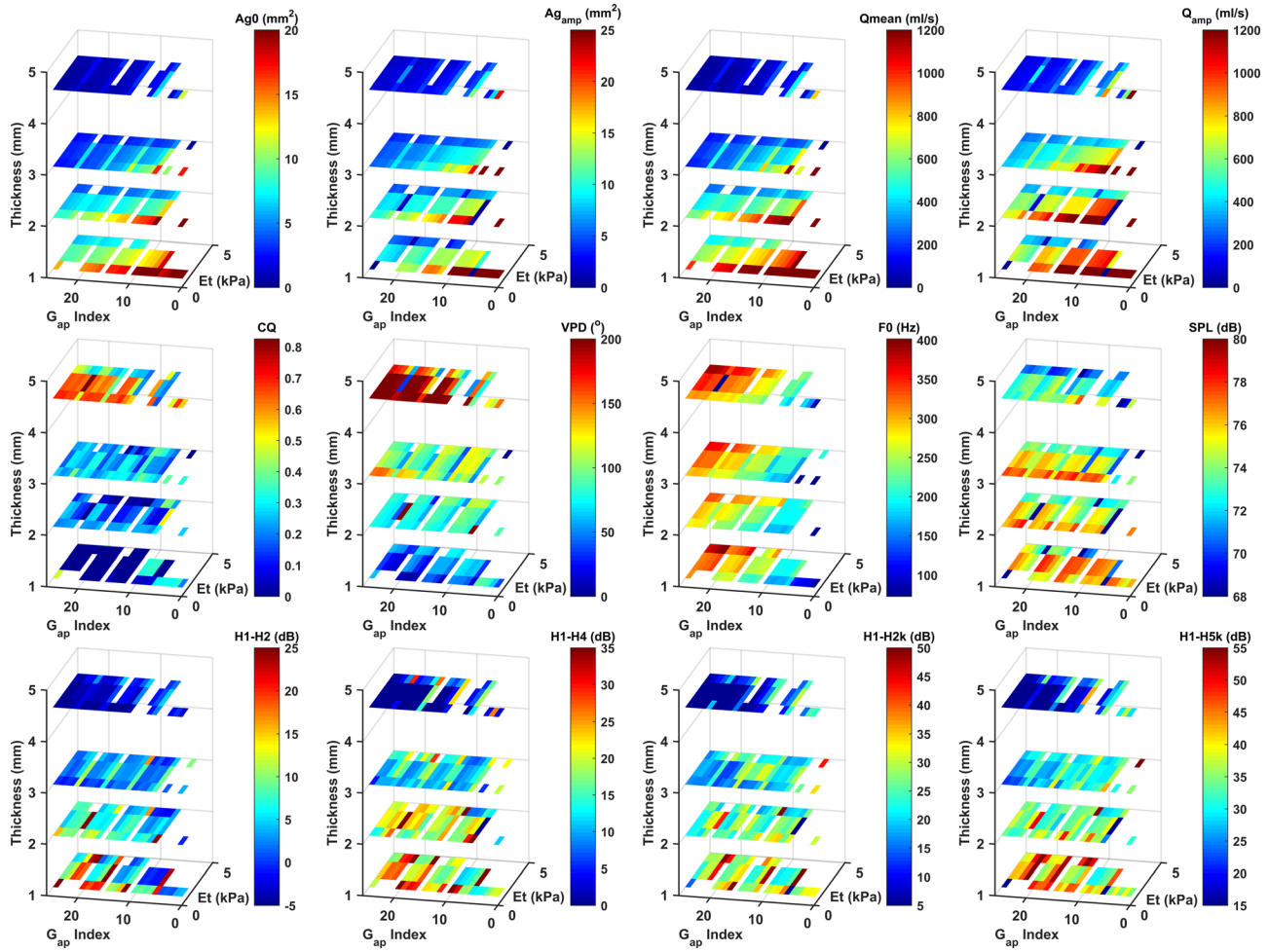

FIG. 4. (Color online) Effects of the transverse stiffness on selected output measures. $P_s = 2$ kPa, $\alpha = 0°$. See Sec. II for definitions of different output measures. The region without data indicates conditions at which no phonation was observed. Note that the G_{ap} index is scaled in such a way so that the AP stiffnesses vary with increasing G_{ap} index in groups of five (Table II), and the effects of increasing body-layer AP stiffness are demonstrated by the within-group variations, whereas the effects of increasing cover-layer AP stiffness are demonstrated by cross-group variations.

which is most obvious for the F0 and sound pressure level (SPL) panels in Fig. 3. Note that only a small part of the first group, which corresponds to conditions with G_{ap} index of 1−5 or $G_{apc} = 1$ kPa, is visible in Fig. 3 because phonation is observed only for a limited conditions within the first group, as discussed in Sec. III A. Again, the effects of increasing body-layer AP stiffness are demonstrated by the within-group variations, whereas the effects of increasing cover-layer AP stiffness are demonstrated by cross-group variations.

Figure 3 shows that increasing AP stiffness in the cover layer significantly reduces the means and amplitudes of both the glottal area and glottal flow rate. A similar effect is also observed for increasing AP stiffness in the body layer, but to a lesser degree. Increasing AP stiffness in the cover layer also increases the phonation frequency F0. The effect of increasing body-layer AP stiffness on F0 is in comparison smaller and less consistent. In general, increasing body-layer AP stiffness increases F0, but may decrease F0 for certain conditions such as thin vocal folds or a large initial glottal gap (e.g., $\alpha = 4°$; not shown in Fig. 3).

In contrast, the effect of increasing AP stiffness on the closed quotient, vertical phase difference, SPL, and the spectral shape is much smaller and less consistent. One exception is for conditions of very small body layer AP stiffness ($G_{apb} = 1$ kPa), in which case increasing G_{apb} leads to significantly increased CQ and VPD and decreased H1−H2, H1−H4, H1−H2k, and H1−H5k. In other words, increasing G_{apb} in these conditions improves glottal closure, reduces H1−H2, and increases excitation of higher-order harmonics. Similar to Zhang (2016), the closed quotient, vertical phase difference, and the spectral shape are primarily controlled by the vertical thickness of the vocal fold.

Figure 4 shows the effects of the transverse Young's modulus E_t on the various output measures, for conditions of Ps = 2 kPa and $\alpha = 0°$. While a 2 kPa subglottal pressure is much higher than typical subglottal pressures in human phonation, it is selected so that phonatory data are available for most of the vocal fold conditions shown. Similar to that of increasing AP stiffness, increasing the transverse stiffness E_t reduces the means and amplitudes of both the glottal area and flow rate, particularly for conditions of small vertical thicknesses. Increasing E_t also increases the phonation frequency, as expected. Unlike that of increasing AP stiffness, increasing E_t has a noticeable effect of reducing CQ and VPD for conditions of large vertical thicknesses, and decreasing SPL. This effect on the CQ and VPD is probably

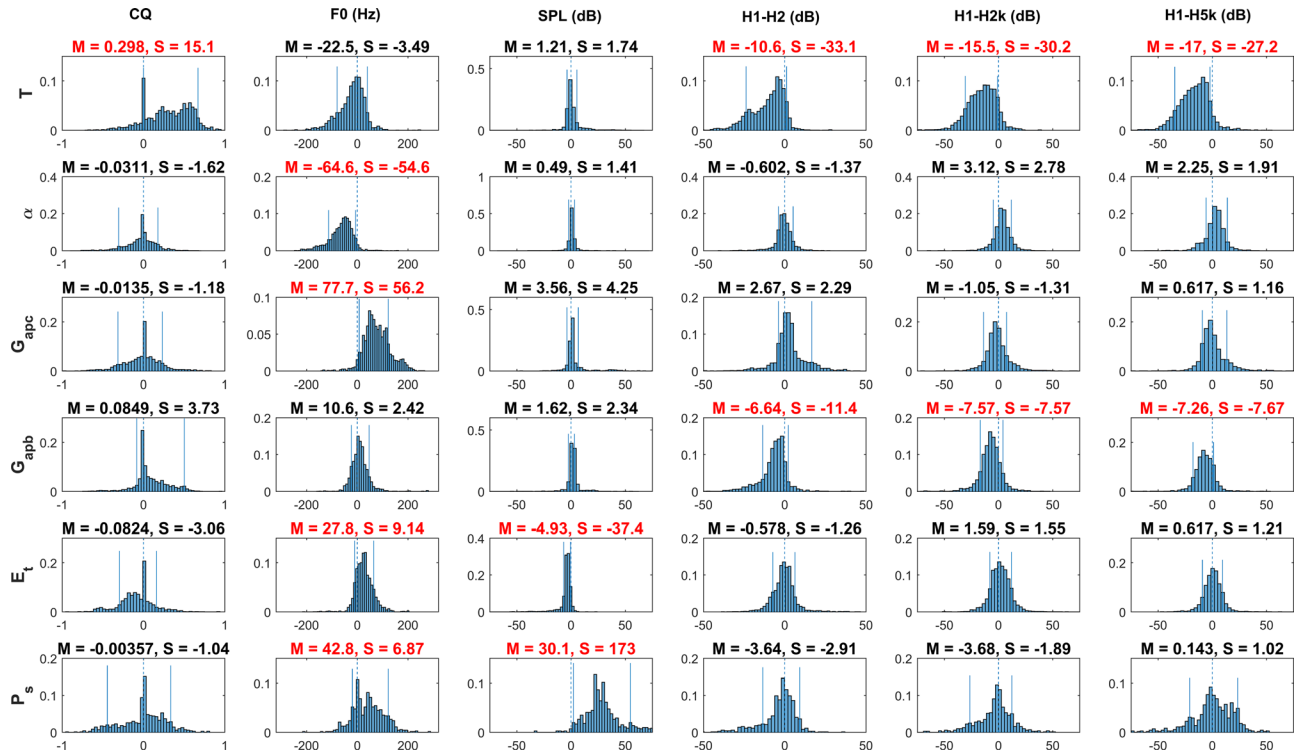

FIG. 5. (Color online) Histograms of changes in selected output measures in response to changes in the six control parameters, all conditions included. In each plot, the dashed line indicates the origin, and the two solid vertical lines mark the region that contains 80% of total sample number. The *M* value quantifies the mean expected change in an output measure due to an increase in a specific control parameter. The *S* value quantifies the likelihood that such output measure is consistently positive or negative across different laryngeal conditions. Important cause−effect pairs that have an absolute *S* value larger than 5 and a dominant absolute *M* value are highlighted.

because increasing E_t increases the wave speed, which reduces the VPD and CQ. A similar effect is observed in lumped-element models with an increased coupling stiffness between the masses (Ishizaka and Flanagan, 1972; Story and Titze, 1995). Increasing E_t also has some effect on the spectral shape, but this effect is less consistent across different vocal fold conditions.

D. Global cause−effect relations: Histogram analysis

Figures 3 and 4 only show a selected small set of vocal fold conditions investigated. To identify important cause−effect relations between physiologic controls and output measures that are consistent across a large range of conditions, histograms are calculated for each of the six control parameters and six selected output measures, as described in Sec. II C. The six selected output measures are the CQ, which plays an important role in linking vocal fold vibration to voice acoustics, and five acoustic measures (F0, SPL, H1−H2, H1−H2k, and H1−H5k) that are perceptually important and can be easily measured from the produced voice signals. These histograms are shown in Fig. 5 for all conditions investigated that produce phonation. As discussed in Sec. II C, a control-output pair has a significant cause−effect relation if both the *M* and *S* factors of the corresponding histogram have large absolute values. In the discussion below, a control parameter is considered to have an important effect on an output measure if the absolute value of the corresponding *S* value is larger than 5 and the absolute *M* value is dominant compared to those of other controls. Cause−effect pairs identified in this way are highlighted in Fig. 5 and summarized in Table III.

The effects of the vertical thickness, resting glottal angle, and the subglottal pressure as identified in Fig. 5 are similar to those identified in Zhang (2016) and are briefly summarized here. The vertical thickness has a dominant effect in CQ and the voice spectral shape (H1−H2, H1−H2k, H1−H5k), thus is responsible for control of spectral shape and higher-order harmonics excitation. Changes in the resting glottal angle have a large effect on F0, whereas varying subglottal pressure has a dominant effect on controlling SPL and a moderate effect on F0.

Regarding the effect of vocal fold stiffness, Fig. 5 shows that two consistent effects of increasing transverse Young's modulus E_t are to increase F0 and slightly decrease SPL. The main effect of increasing cover-layer AP stiffness is to increase F0, and this is one of the most effective mechanisms of increasing F0, comparing the *M* value of G_{apc} to those of other controls. The primary effect of increasing body-layer AP stiffness G_{apb} that is consistent over a large range is to reduce H1−H2, H1−H2k, and H1−H5k, although this effect is smaller and less consistent than that of the vertical thickness.

Figures 3 and 4 show that the effect of G_{apb} on regulating the spectral shape is mostly limited to conditions of very small G_{apb}. Considering that during phonation the AP stiffness in the body is likely to be larger than that in the cover layer, the histogram analysis is repeated, excluding conditions with $G_{apb} < G_{apc}$ which may not be physiologically realistic, and

TABLE III. Summary of significant cause–effect relation that is consistent across all vocal fold conditions (as shown in Fig. 5). ++, strong and consistently positive effect; −−, strong and consistently negative effect. * denotes cause–effect pairs that are no longer significant or consistent when vocal fold conditions with $G_{apb} < G_{apc}$ are excluded from consideration. Symbols in parentheses indicate cause–effect relation that is consistent and significant only when vocal fold conditions with $G_{apb} < G_{apc}$ are excluded from consideration (as shown in Fig. 6).

	CQ	F0 (Hz)	SPL (dB)	H1−H2 (dB)	H1−H2k (dB)	H1−H5k (dB)
T (mm)	+ +			− −	− −	− −
α (°)		− −				
G_{apc} (kPa)		+ +	(+ +)			
G_{apb} (kPa)				− −*	− −*	− −*
E_t (kPa)		+ +	− −			
P_s (kPa)		++*	+ +			

the results are shown in Fig. 6. With the conditions of $G_{apb} < G_{apc}$ excluded, no important cause–effect relation is identified in Fig. 6 for the body-layer AP stiffness. On the other hand, the cover-layer AP stiffness $G_{apc,}$ which now combines the effects of G_{apb} and $G_{apc,}$ exhibits a small but consistent effect in regulating SPL.

IV. DISCUSSION AND CONCLUSIONS

As expected, changes in vocal fold stiffness play an important role in F0 control. In addition, changes in vocal fold stiffness also have a large impact on the phonation threshold pressure and the glottal area and flow rate, with increasing stiffness reducing the means and amplitudes of both the glottal area and flow rate. In contrast, the effect of varying vocal fold stiffness on the closed quotient, vertical phase difference of vocal fold vibration, and the spectral slope of the output acoustics is much smaller and inconsistent. This is particularly the case when conditions with G_{apb} smaller than $G_{apc,}$ which are physiologically less realistic, are excluded from consideration. Similar to Zhang (2016), this study shows that the CQ and the spectral shape of the output acoustics are primarily controlled by the vertical thickness of the medial surface T.

The effect of vocal fold AP stiffness on the glottal area waveform was briefly studied by Titze and Talkin (1979) using a three-dimensional continuum model. Although the effect of stiffness on glottal closure and the output voice spectra was not explicitly investigated, their results (Fig. 3 in Titze and Talkin, 1979) do not appear to show much effect of the AP stiffness on the shape of the glottal area waveform, which is consistent with the findings of the present study.

The body-cover theory of phonation (Hirano, 1974; Hirano and Kakita, 1985) argues that different voice types

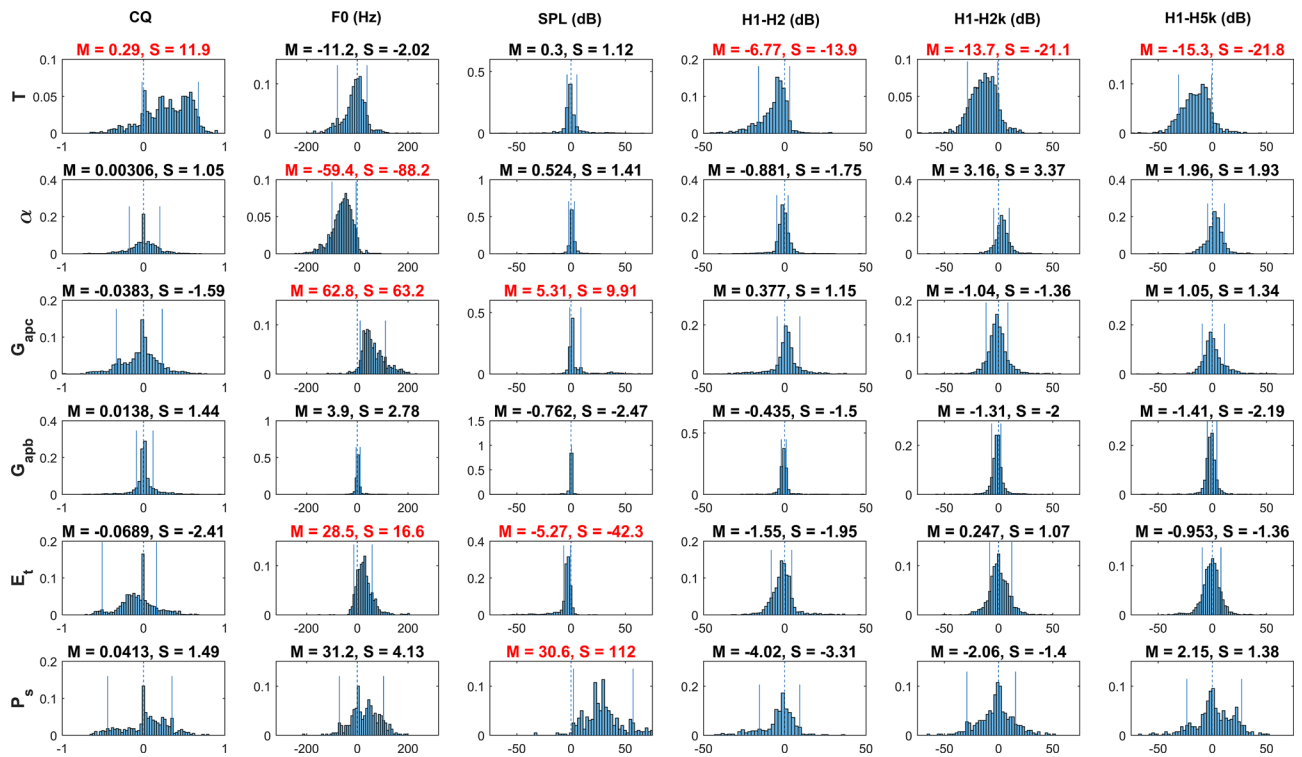

FIG. 6. (Color online) Histograms of changes in selected output measures in response to changes in the six control parameters, excluding conditions in which $G_{apb} < G_{apc}$. In each plot, the dashed line indicates the origin, and the two solid vertical lines mark the region that contains 80% of total sample number. The M value quantifies the mean expected change in an output measure due to an increase in a specific control parameter. The S value quantifies the likelihood that such output measure is consistently positive or negative across different laryngeal conditions. Important cause–effect pairs that have an absolute S value larger than 5 and a dominant absolute M value are highlighted.

are associated with different stiffness conditions within the body and cover layers. Although the transverse and AP stiffnesses are not clearly distinguished in the body-cover theory (they were collectively referred to as elastic constants), the discussion of control of vocal fold length and longitudinal tension by activation of the CT/TA muscles (Hirano, 1974; Hirano and Kakita, 1985) implies that a significant difference among the four voice types is the differential AP stiffness in the body and cover layers. This may seem to contradict the small effect of varying vocal fold AP stiffness on CQ, VPD, and the spectral shape of output acoustics observed in the present study. However, it should be noted that in the present study vocal fold stiffness, vocal fold geometry, and the resting glottal angle are all control parameters independent of each other. In humans, because vocal fold geometry and stiffness are controlled by the same set of laryngeal muscles (the CT and TA muscles; Hirano, 1988; Vahabzadeh-Hagh *et al.*, 2017), changes in vocal fold stiffness are often accompanied by changes in geometry (e.g., vertical thickness) that play an important role in regulating voice types. Thus, although there is no direct cause−effect relation between vocal fold stiffness and voice types, as demonstrated in this study, because of this physiological correlation in the control of stiffness and geometry, a strong correlation between vocal fold stiffness and voice types may still occur during human phonation.

Although the body-cover difference in AP stiffness has a relatively small effect on the spectral shape of the produced sound, the body-cover structure of the vocal folds has an important role in vocal fold posturing and voice control, including for example a finer control of vocal fold AP stiffness (thus a finer F0 control) by an antagonistic pair of muscles than by a single muscle, better control of membranous vocal fold approximation, and improved glottal closure through increased vertical thickness. Computationally, this small effect of body-cover AP stiffness differential on the spectral slope of the output voice indicates that vocal folds may be modelled as a one-layer structure, which would significantly reduce the number of material properties control parameters and computational complexity in models of voice production, provided that vocal fold posturing is properly modeled so that the physiological correlation between changes in vocal fold stiffness, geometry, and position is preserved.

One limitation of this study is that the transverse stiffness is set to be identical in the body and cover layers, which may be partially responsible for the small effect of varying transverse stiffness on glottal closure and the output voice spectra. It is possible a larger effect may be observed when the body-cover difference in the transverse stiffness is varied in a larger range. For example, Story and Titze (1995) showed in their three-mass model that the body-cover ratio in the spring constants, when varied in a large range, can have a large effect on the vertical phase difference, which is critically related to the glottal closure pattern and voice spectral shape (Zhang, 2016). Because the three-mass model describes vocal fold motion in the coronal plane, their findings suggest a possibly important role of the body-cover difference in the transverse stiffness in regulating vertical phase difference. However, direct translation of the findings in lumped-element models to a three-dimensional setting is difficult. Because of the neglect of physics along the AP dimension, the spring constants in lumped-element models must play the role of both the transverse and AP stiffnesses (e.g., a large range of variation in the spring constants is required in order to produce a F0 range typical of humans). Indeed, while the stiffness constants in lumped-element models are better related to the transverse stiffness in a three-dimensional model, the large range of variation of these spring constants in lumped-element models is often based on experimental data of the AP stiffness of the vocal folds (e.g., Titze and Story, 2002). Unfortunately, currently there are no experimental data regarding the range of body-cover difference in the transverse stiffness during normal human phonation. In the present study, besides the obvious need to reduce the number of parametric conditions, the simplification of imposing identical body-cover transverse stiffness is based on the numerical finding of Yin and Zhang (2013) which, using experimentally measured passive and active material properties of the vocal folds, showed that the transverse stiffnesses of the body and cover layers are generally of the same order of magnitude across all CT/TA muscle activation conditions. In other words, the body-cover difference in the transverse stiffness during normal human phonation is less likely to vary in a large range as investigated in lumped-element models (e.g., Story and Titze, 1995). Nevertheless, the effect of body-cover differences in the transverse stiffnesses is worth further investigation, particularly when experimental data become available regarding the range of transverse stiffness within different layers during human phonation.

ACKNOWLEDGMENTS

This study was supported by research Grant Nos. R01 DC001797 and R01 DC011299 from the National Institute on Deafness and Other Communication Disorders, the National Institutes of Health.

Alipour, F., Berry, D. A., and Titze, I. R. (**2000**). "A finite-element model of vocal-fold vibration," J. Acoust. Soc. Am. **108**, 3003−3012.

Berry, D. A. (**2001**). "Mechanisms of modal and nonmodal phonation," J. Phon. **29**, 431−450.

Berry, D. A., Herzel, H., Titze, I. R., and Krischer, K. (**1994**). "Interpretation of biomechanical simulations of normal and chaotic vocal fold oscillations with empirical eigenfunctions," J. Acoust. Soc. Am. **95**, 3595−3604.

Farahani, M., and Zhang, Z. "Experimental validation of a three-dimensional reduced-order continuum model of phonation," J. Acoust. Soc. Am. **140**, EL172−EL177 (**2016**).

Gray, S. D. (**2000**). "Cellular physiology of the vocal folds," Otolaryngol. Clin. North Am. **33**(4), 679−697.

Hirano, M. (**1974**). "Morphological structure of the vocal fold and its variations," Folia Phoniatr. **26**, 89−94.

Hirano, M. (**1988**). "Vocal mechanisms in singing: Laryngological and phoniatric aspects," J. Voice **2**, 51−69.

Hirano, M., and Kakita, Y. (**1985**). "Cover-body theory of vocal fold vibration," in *Speech Science: Recent Advances*, edited by R. G. Daniloff (College-Hill Press, San Diego), pp. 1−46.

Ishizaka, K., and Flanagan, J. L. (**1972**). "Synthesis of voiced sounds from a two-mass model of the vocal cords," Bell Syst. Tech. J. **51**, 1233−1267.

Itskov, M., and Aksel, N. (**2002**). "Elastic constants and their admissible values for incompressible and slightly compressible anisotropic materials," Acta Mech. **157**, 81–96.
Klatt, D. H., and Klatt, L. C. (**1990**). "Analysis, synthesis and perception of voice quality variations among male and female talkers," J. Acoust. Soc. Am. **87**, 820–856.
Murray, P. R., and Thomson, S. L. (**2012**). "Vibratory responses of synthetic, self-oscillating vocal fold models," J. Acoust. Soc. Am. **132**, 3428–3438.
Pelorson, X., Hirschberg, A., Van Hassel, R. R., Wijnands, A. P. J., and Auregan, Y. (**1994**). "Theoretical and experimental study of quasisteady-flow separation within the glottis during phonation. Application to a modified two-mass model," J. Acoust. Soc. Am. **96**(6), 3416–3431.
Story, B. H., and Titze, I. R. (**1995**). "Voice simulation with a body-cover model of the vocal folds," J. Acoust. Soc. Am. **97**, 1249–1260.
Thomson, S. L., Mongeau, L., and Frankel, S. H. (**2005**). "Aerodynamic transfer of energy to the vocal folds," J. Acoust. Soc. Am. **118**, 1689–1700.
Titze, I., and Story, B. H. (**2002**). "Rules for controlling low-dimensional vocal fold models with muscle activation," J. Acoust. Soc. Am. **112**, 1064–1076.
Titze, I., and Talkin, D. (**1979**). "A theoretical study of the effects of various laryngeal configurations on the acoustics of phonation," J. Acoust. Soc. Am. **66**, 60–74.
Vahabzadeh-Hagh, A., Zhang, Z., and Chhetri, D. (**2017**). "Three-dimensional posture changes of the vocal fold from paired intrinsic laryngeal muscles," Laryngoscope **127**, 656–664.
van den Berg, J. W. (**1968**). "Register problems," Ann. N.Y. Acad. Sci. **155**(1), 129–134.
van den Berg, J. W., and Tan, T. S. (**1959**). "Results of experiments with human larynxes," Pract. Otorhinolaryngol. **21**, 425–450.
White, F. M. (**1991**). *Viscous Fluid Flow*, 2nd ed. (McGraw-Hill, New York), p. 119.
Wu, L., and Zhang, Z. (**2016**). "A parametric vocal fold model based on magnetic resonance imaging," J. Acoust. Soc. Am. **140**, EL159–EL165.
Xuan, Y., and Zhang, Z. (**2014**). "Influence of embedded fibers and an epithelium layer on glottal closure pattern in a physical vocal fold model," J. Speech, Lang., Hear. Res. **57**, 416–425.
Yin, J., and Zhang, Z. (**2013**). "The influence of thyroarytenoid and cricothyroid muscle activation on vocal fold stiffness and eigenfrequencies," J. Acoust. Soc. Am. **133**, 2972–2983.
Zhang, Z. (**2009**). "Characteristics of phonation onset in a two-layer vocal fold model," J. Acoust. Soc. Am. **125**, 1091–1102.
Zhang, Z. (**2010**). "Dependence of phonation threshold pressure and frequency on vocal fold geometry and biomechanics," J. Acoust. Soc. Am. **127**, 2554–2562.
Zhang, Z. (**2015**). "Regulation of glottal closure and airflow in a three-dimensional phonation model: Implications for vocal intensity control," J. Acoust. Soc. Am. **137**, 898–910.
Zhang, Z. (**2016**). "Cause–effect relationship between vocal fold physiology and voice production in a three-dimensional phonation model," J. Acoust. Soc. Am. **139**, 1493–1507.
Zhang, Z., and Luu, T. (**2012**). "Asymmetric vibration in a two-layer vocal fold model with left-right stiffness asymmetry: Experiment and simulation," J. Acoust. Soc. Am. **132**(3), 1626–1635.
Zhang, Z., Mongeau, L., and Frankel, S. H. (**2002**). "Experimental verification of the quasi-steady approximation for aerodynamic sound generation by pulsating jets in tubes," J. Acoust. Soc. Am. **112**(4), 1652–1663.
Zhang, Z., Neubauer, J., and Berry, D. A. (**2006**). "The influence of subglottal acoustics on laboratory models of phonation," J. Acoust. Soc. Am. **120**(3), 1558–1569.